Femtosecond Time-Resolved CARS Spectroscopy on Binary Gas-Phase Mixtures: A Theoretical and Experimental Study of the Benzene/Toluene System

6 AUTHORS, INCLUDING:

Oliver Rubner
University of Münster
32 PUBLICATIONS **417** CITATIONS

SEE PROFILE

Gregor Knopp
Paul Scherrer Institut
80 PUBLICATIONS **744** CITATIONS

SEE PROFILE

Arnulf Materny
Jacobs University
198 PUBLICATIONS **2,328** CITATIONS

SEE PROFILE

Wolfgang Kiefer
University of Wuerzburg
878 PUBLICATIONS **9,837** CITATIONS

SEE PROFILE

Femtosecond Time-Resolved CARS Spectroscopy on Binary Gas-Phase Mixtures: A Theoretical and Experimental Study of the Benzene/Toluene System

O. Rubner, M. Schmitt, G. Knopp, A. Materny, W. Kiefer, and V. Engel*

Institut für Physikalische Chemie, Universität Würzburg, Am Hubland, 97074 Würzburg, Germany

Received: August 4, 1998; In Final Form: September 23, 1998

Femtosecond time-resolved CARS measurements on benzene, toluene, and binary mixtures of these molecules have been performed in the gas phase. Whereas a two-pulse excitation process prepares benzene in a single vibrational state, a vibrational wave packet is excited in toluene, which gives rise to oscillatory patterns in the CARS signal. For the mixed system one finds beats between modes coherently excited in both molecules. The results are analyzed using perturbative quantum calculations. It is shown that the rotational degree of freedom is responsible for the decay of the CARS signal in all cases. Furthermore, it is demonstrated that the details of the excitation process have to be incorporated in the calculation to obtain the correct amplitudes of the oscillating signals.

1. Introduction

The technique of time-domain spectroscopy to observe the internal dynamics of molecules or the course of chemical reactions has been applied to a great variety of systems.[1−5] Besides pump/probe fluorescence, transient absorption, or ionization techniques, nonlinear spectroscopic methods have become a valuable tool to investigate the dynamic properties of molecules.[6] Since Leonhardt et al.[7,8] applied femtosecond laser pulses to the observation of time-resolved coherent anti-Stokes Raman scattering (CARS) several groups have reported subpicosecond time-resolved CARS measurements.[9−15] Time-resolved coherent Raman scattering techniques have been widely employed in condensed-phase studies of vibrational dephasing and molecular orientational motion.[7,8,16−26] However, these methods have not been exploited on the subpicosecond time scale for gas-phase studies until recently. Hayden and Chandler[15] reported the application of femtosecond time-resolved coherent Raman techniques to excite and monitor the evolution of vibrational coherences in gas-phase samples of benzene as well as 1,3,5-hexatriene. From their experiments, they conclude that in the case of benzene the thermal averaging over many rotational contributions oscillating with different frequencies causes the overall decay of the time-resolved CARS signal. In contrast to this, in 1,3,5-hexatrien, the rotation of the molecules away from their initial spatial orientation is primarily responsible for the coherence decay.

Theories to describe time-resolved nonlinear spectroscopical measurements were developed by several researchers.[27−34] Most descriptions use the formalism of density matrixes,[6] which is appropriate for molecules in liquid or solid environments. Since in the present paper we treat only gas-phase systems, we are not forced to adopt a density matrix approach and can simply work with state vectors.[35]

The paper is organized as follows. Section 2 contains a brief description of our experiments. The general theory is summarized in Section 3, and Section 4 presents the results. Finally, a short summary is given in Section 5.

2. Experimental Section

The experimental apparatus for measuring time-resolved CARS in a folded "boxcars" geometry has been described in detail elsewhere.[36−38] Briefly, a Ti:Sapphire laser system in combination with two four-pass OPAs was used to create the three femtosecond pulses. The pulses had energies of a few microjoules and pulse durations of typically 80 fs. The output of one OPA was split into two equal parts by means of a 50/50 beam splitter to provide the two pump pulses, which are characterized by their frequencies, ω_1 and ω_2, and wave vectors, k_1 and k_2. The output from a second OPA was used as the Stokes pulse. All three laser beams were made parallel and then focused into the sample cell by an achromatic lens. The folded boxcars configuration was employed in order to separate the signal from the incoming beams.[39] In this geometry the phase-matching condition is fulfilled. The pulses were delayed relative to each other by means of Michelson interferometer arrangements. In the experiments presented in this paper, two laser pulses were kept temporally overlapped and fixed. They were used for Raman excitation of the sample by tuning the frequency difference to a vibrational Raman transition in the molecules. The coherent excitation was monitored by the interaction with the probe pulse of frequency ω_1' and wave vector k_1'. The anti-Stokes radiation generated by the probing process was detected by a fast photomultiplier tube after it was spatially and spectrally filtered by means of pinholes and a monochromator, respectively. The coherent signal was recorded as a function of the delay time T between the exciting pump and probe pulses.

In this contribution, we report results obtained by means of femtosecond time-resolved CARS spectroscopy on benzene, toluene, and their binary mixtures in the gas phase. The sample cell containing liquid benzene, toluene, or a 1:1 mixture of both was heated to ∼80 °C. For this temperature, the vapor pressure of benzene was approximately 1000 hPa, and that of toluene was about 500 hPa. Therefore, the ratio of the gaseous mixture of benzene and toluene was about 2:1.[40] Benzene and toluene samples were used as received (Aldrich).

For the Raman excitation, a frequency difference of $(\omega_1 - \omega_2)/(2\pi c) = 1000$ cm^{-1} between the pump and the Stokes lasers was chosen. As a result of the spectral width of the femtosecond exciting lasers of more than 200 cm^{-1}, several modes were simultaneously excited in the molecules; the Raman active vibrations of benzene at wavenumber positions 991 and 984
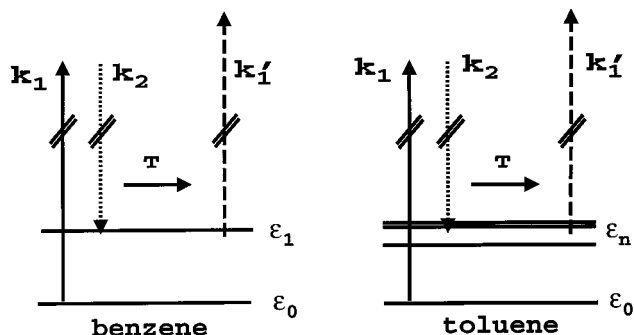
Figure 1. Excitation scheme for benzene and toluene. A single term contributing to the third-order polarization is displayed for each case. The horizontal lines belong to energies of vibrational states that participate in the Raman process. The fields are noted by their wave vectors $\mathbf{k}_1$, $\mathbf{k}_1'$ (absorption), and $\mathbf{k}_2$ (emission). The lengths of the arrows do not reflect the peak frequencies of the pulses.

cm^{-1} can be assigned to the ring-breathing mode of benzene[41] and of benzene with one carbon-13 present at natural abundance.[21] The wavenumbers of the excited Raman transitions in toluene are 788, 1001, and 1028 cm^{-1}. These can be assigned to the ring-breathing mode and ring-deformation modes of toluene, respectively (see ref 41 and references in therein).

3. Theory

The simulation of the time-resolved CARS signals requires the calculation of the third-order polarization induced in pure benzene or toluene samples and in a mixture of these molecules. We will treat the interaction of the molecular samples with three femtosecond pulses within perturbation theory and restrict our treatment to gas-phase samples under collision-free conditions.

Let us first discuss a pure ensemble of molecules. The polarization in the case of optically thin media is given by the expectation value of the dipole moment $\boldsymbol{\mu}$

$$\mathbf{P}(t) = \langle \psi(t)|\boldsymbol{\mu}|\psi(t)\rangle \qquad (1)$$

where $\psi(t)$ is the time-dependent state vector of the system.

The electric fields can be written as

$$\mathbf{E}_1(t) = \mathbf{E}f_1(t)\, e^{-i\omega_1 t}\, e^{i\mathbf{k}_1\mathbf{x}} + cc \qquad (2)$$

$$\mathbf{E}_2(t) = \mathbf{E}f_2(t)\, e^{-i\omega_2 t}\, e^{i\mathbf{k}_2\mathbf{x}} + cc \qquad (3)$$

and

$$\mathbf{E}_1'(t) = \mathbf{E}f_1(t-T)\, e^{-i\omega_1(t-T)}\, e^{i\mathbf{k}_1'\mathbf{x}} + cc \qquad (4)$$

Here $\mathbf{E}$ denotes the polarization vector, which is the same for all fields. $f(t)$ is the pulse envelope function centered around $t = 0$ (for $\mathbf{E}_1$ and $\mathbf{E}_2$) and at the delay time T (for $\mathbf{E}_1'$). In our case, the fields $\mathbf{E}_1$ and $\mathbf{E}_2$ act simultaneously with the molecules, whereas the third pulse $\mathbf{E}_1'$ is time-delayed. The polarization emitted in direction $\mathbf{k}_1 - \mathbf{k}_2 + \mathbf{k}_1'$ consists of several contributions of different relative magnitude. Within perturbation theory, all terms can be determined. As an example we discuss one contribution $\mathbf{P}_{03}(t)$ in what follows. The corresponding excitation scheme is displayed in Figure 1; the first two pulses ($\mathbf{k}_1$, $\mathbf{k}_2$) prepare a second-order state that evolves in time. This state serves as the initial state for the interaction with the third pulse ($\mathbf{k}_1'$). We then have to calculate the projection on the initial state $|i\rangle$

$$\mathbf{P}_{03}(t) = 2\, \mathrm{Re}\langle i|\mu|\psi^{(3)}(\mathbf{k}_1 - \mathbf{k}_2 + \mathbf{k}_1')\rangle \qquad (5)$$

In more detail, the third-order state is (atomic units are used throughout)

$$|\psi(\mathbf{k}_1 - \mathbf{k}_2 + \mathbf{k}_1',t)\rangle \approx \int_{-\infty}^{t} dt_3\, U(t - t_3)\boldsymbol{\mu}\mathbf{E}_1'(t_3) \times$$
$$\int_{-\infty}^{t_3} U(t_3 - t_2)\boldsymbol{\mu}\mathbf{E}_2(t_2) \int_{-\infty}^{t_2} dt_1 U(t_2 - t_1)\boldsymbol{\mu}\mathbf{E}_1(t_1)U(t_1)\, |i\rangle \quad (6)$$

where $U(t) = e^{-iHt}$ is the propagator containing the Hamiltonian, H.

In our calculations, we simulate the vibrational degrees of freedom via an $(N + 1)$-level system. Here N vibrational states $|n\rangle$ of energy ϵ_n in the electronic ground state (g) and a single level $|e\rangle$ in an electronically excited state (e) are taken into account. Starting from the vibrational ground state ($n = 0$) and a rotational state with a set of quantum numbers (α), the initial state is $|i\rangle = |0,\alpha\rangle$ and the above state vector can be written as

$$|\psi(\mathbf{k}_1 - \mathbf{k}_2 + \mathbf{k}_1',t)\rangle = \int_{-\infty}^{t} dt_3 \int_{-\infty}^{t_3} dt_2 \int_{-\infty}^{t_2} dt_1\, f_1'(t_3 - T) \times$$
$$f_2(t_2) f_1(t_1) e^{-i\omega_1(t_3 - T)}\, e^{+i\omega_2 t_2}\, e^{-i\omega_1 t_1} \sum_{n}\sum_{\beta''}\sum_{\beta'}\sum_{\beta} |e,\beta''\rangle \times$$
$$\langle e,\beta''|\boldsymbol{\mu}_{eg}\mathbf{E}|n,\beta'\rangle\langle n,\beta'|\boldsymbol{\mu}_{eg}\mathbf{E}|e,\beta\rangle\langle e,\beta|\boldsymbol{\mu}_{eg}\mathbf{E}|0,\alpha\rangle\, a_e(t - t_3) \times$$
$$a_{\beta''}(t - t_3)\, a_n(t_3 - t_2)\, a_{\beta'}(t_3 - t_2)\, a_e(t_2 - t_1)\, a_\beta(t_2 - t_1) \times$$
$$a_0(t_1)\, a_\alpha(t_1) \quad (7)$$

Here we have introduced the notation $a_l(s) = e^{-i\epsilon_l s}$ and assumed the separation of vibrational and rotational degrees of freedom and the completeness of the expansions. β, β', and β'' are rotational quantum numbers, and $\boldsymbol{\mu}_{eg}$ is the transition dipole moment between the electronic states. The dependence of the fields on the spatial coordinate $\mathbf{x}$ was neglected within the dipole approximation. Similar equations are obtained for the state vectors that enter into the calculation of other terms contributing to the total polarization.

The pump/probe CARS signal is obtained as

$$S(T) = \int_{-\infty}^{T + \tau} dt\, |\mathbf{P}(t)|^2 \qquad (8)$$

where τ is the time the third pulse stopped interacting with the system and we denoted the delay time, T, explicitly.

To simulate the experiments we have to account for the thermal initial distribution of the molecules. The contribution of thermally populated higher vibrational states is negligible so that we have to take only rotational states into account. Thus, we determine the polarization $\mathbf{P}_\alpha(t)$ for a set of rovibrational initial states $|i\rangle = |0,\alpha\rangle$. Since every molecule in the statistical mixture emits radiation that is detected in the $\mathbf{k}_1 - \mathbf{k}_2 + \mathbf{k}_1'$ direction, the contributions from different initial rotational states to the polarization have to be added coherently

$$\mathbf{P}(t) = \sum_{\alpha} b_\alpha \mathbf{P}_\alpha(t) \qquad (9)$$

where b_α are Boltzmann factors.

In a mixture of different molecules γ with relative concentrations c_γ, a polarization $\mathbf{P}_{\alpha\gamma}(t)$ is induced in each molecule and as above the total radiation emitted from the sample is a coherent superposition of all fields:

$$\mathbf{P}(t) = \sum_{\gamma} c_\gamma \sum_{\alpha} b_{\alpha\gamma} \mathbf{P}(t) \qquad (10)$$

We now turn to the time-resolved CARS spectroscopy of benzene and toluene.

4. Results

4.a. Gas-Phase Benzene. The excitation scheme for benzene, as depicted in Figure 1, shows that a single vibrational level $n = 1$ is excited. This is due to our laser pulses that have a temporal width (full width at half-maximum, fwhm) of 80 fs and peak frequencies corresponding to energies of 2.254 and 2.13 eV. With these parameters, only the ring-breathing mode can be excited, which lies at 991 cm^{-1} (0.123 eV) in benzene and at 984 cm^{-1} (0.122 eV) in $^{13}C^{12}C_5H_6$. We treat nonresonant excitation proceeding via the perpendicular transition ($A^1B_{2u} \leftarrow X^1A_{1g}$) electronic transition, which is allowed due to vibronic coupling.[42]

The general equations for the polarization have to be specialized for the symmetric top molecule benzene. Let us again discuss the contribution $\mathbf{P}_{03}(t)$ as an example. First of all, the sum over n vanishes in the expression for the state vector (eq 7). The matrix elements as a function of the symmetric top quantum numbers J and K can be evaluated analytically using angular momentum algebra.[43] Here we will perform this calculation only approximately. In doing so, we treat the limit where K is equal to J, which is appropriate for an oblate symmetric top. One finds transitions with $\Delta K = \pm 1$ and $\Delta J = 0$ and ± 1, and the Hönl−London factors for these transitions are readily available.[43] The rotational energies are consequently approximated as

$$\epsilon_{JK} = AJ^2 + (A - C)K^2 \approx (2A - C)J^2 \qquad (11)$$

where A and C are the moments of inertia of the symmetric top.

The state vectors are determined numerically. Note that the selection rules that follow from the angular integrals reduce the sums over β, β', and β'' to only a few terms.

Figure 2a displays the calculated signal for an initial rotational state of $^{12}C_6H_6$ with $J = K = 18$, which corresponds to the maximum of the rotational intensity distribution at the temperature $T = 345$ K. Here and in what follows, we do not treat the case when all three pulses overlap temporarily. We find several beats corresponding to the rotational energy differences as described in the theoretical part. After the first decay due to the rotational dephasing, there is a revival of the signal at about 25 ps. If the initial states are averaged according to the Boltzmann distribution, a decay of the signal is obtained. The decay however is not monotonic, and a plateau is found between 2 and 6 ps. For longer times, the calculated signal does not exhibit a revival rather the intensity remains zero.

The curve in Figure 2c shows the signal obtained from a mixture of 94% $^{12}C_6H_6$ and 6% $^{13}C^{12}C_5H_6$ according to the natural abundance of ^{13}C. A comparison with Figure 2b shows that an additional structure appears that is obviously due to an isotope effect. Indeed, the time difference between the two minima corresponds to a beat frequency between the two vibrational modes that are excited in the two isotopes. This effect will be discussed in more detail in Section 4.c.

The measured CARS signal is displayed in Figure 2d. A comparison with theory (Figure 2c) shows that the agreement is reasonably good. The decay as well as the plateau is aparent in both curves, although the second peak that occurs around 6 ps in the theoretical curve is not found experimentally. The calculated signal decays more slowly, which is due to the
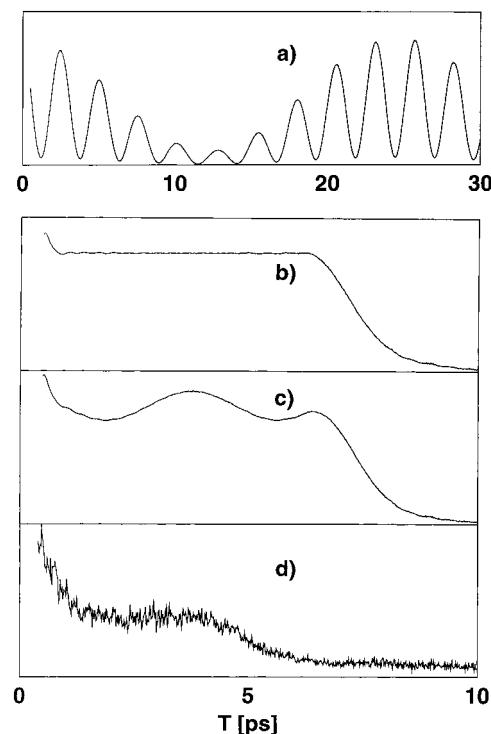
Figure 2. Time-resolved CARS signals for benzene: (a) calculated signal for a single initial rotational state $J = K = 18$; (b) contains the rotational averaged calculated signal for pure benzene; (c) includes the isotopic species $^{13}C^{12}C_6H_6$; (d) experiment.

neglecting of initial rotational states with a K quantum number different from J.

4.b. Gas-Phase Toluene. A different situation than that for benzene is encountered in the toluene system, as can be seen in the excitation scheme (right diagram in Figure 1). The same parameters were used for the laser fields. In this case, several vibrational levels can be excited coherently through the interaction with the first two laser pulses. The preparation of a vibrational wave packet composed of several eigenstates for the vibrational degrees of freedom results in quantum beats in the CARS signal, as can be seen in Figure 3a, which shows the theoretical signal including only the vibrational degree of freedom. Several oscillations appear that clearly belong to the input of the calculation, that is, to vibrational energy differences in the toluene molecule. The signal does not exhibit any decay and will oscillate with the same amplitudes for infinite times. As for benzene, the rotational degree of freedom has to be included to obtain a proper description. Although toluene is an asymmetric rotor, we treat it as a symmetric rotor. In this case it is a prolate symmetric top, and we might calculate the rotational line intensities in the limit that J is much larger than K; that is, we take $K = 0$ so that the rotational energies are given by

$$\epsilon_{JK} = AJ^2 + (A - C)K^2 \approx AJ^2 \qquad (12)$$

The rotational constants of toluene are 8.110^{-5}, 3.710^{-5}, and 2.610^{-5} eV, respectively. Thus, a symmetric top approximation can be justified as the lower two values are comparable. Yet it can be expected that this approximation leads to a slower decay of the CARS signal because we neglect some of the energy differences of the asymmetric top. Furthermore, we have to note that the approximation $K = 0$ is rather crude, since many contributions from different K values are neglected.

Figure 3b shows the simulated signal, which now includes the rotations within the approximations mentioned above. The

CARS Spectroscopy on Binary Gas-Phase Mixtures

*J. Phys. Chem. A, Vol. 102, No. 48, 1998* **9737**
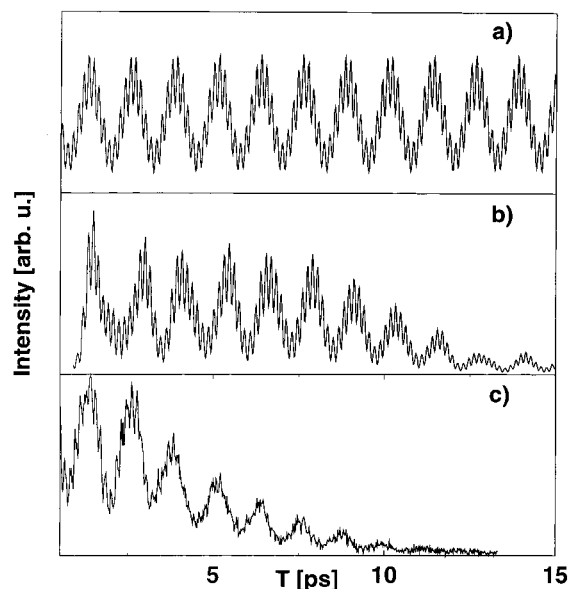
Figure 3. Time-resolved CARS signals for toluene. Theoretical signals are shown for calculations without rotations (a) and taking rotations into account (b). The lower panel (c) displays the experimental signal.

Figure 4. Time-resolved CARS signals for a mixture of toluene and benzene. The theoretical signals in (a) and (b) were obtained using slightly different vibrational energies for toluene, as described in the text. The experimental signal is shown in (c).

signal decays due to the averaging over many rotational states. In the present case, we did not include isotopes of toluene in the calculation. Since the signals exhibit very strong structures, the isotope effect will however not be significant in the present case.

The calculated signal decays slower than the experimental one, which is displayed in Figure 3c. This is due to our approximation in the description of the rotational level structure of the molecule. Nevertheless, the agreement between theory and experiment is satisfactory. In passing, we note that the amplitudes of the temporal variations are sensitive to the actual description of the excitation process, i.e., the pulse parameters such as width or frequency.

4.c. Gas-Phase Benzene/Toluene Mixtures. Let us now discuss mixtures of benzene and toluene under gas-phase conditions. Since each molecule in the mixture irradiates an electromagnetic field, the sum of these fields consists of a coherent sum of the induced polarizations of all the components. This opens the possibility to observe beats between modes in the different molecules,[7,8,12] which are sometimes called polarization beats.[44] Figure 4a shows the calculated time-resolved CARS signal for a mixture of 80% benzene and 20% toluene. Here, we used vibrational energies (all values in electronvolts) of 0.0977, 0.1241, 0.1275 (toluene), 0.1229 ($^{12}C_6H_6$), and 0.1218 for $^{13}C^{12}C_5H_6$. The appearance of the signal now is quite different from what is found in the case of pure benzene or toluene samples. From a Fourier analysis, we find the vibrational frequncies of toluene and additionally a frequency that belongs to the energy difference between the modes most strongly excited in benzene and toluene. A second theoretical signal is displayed in Figure 4b. Here, we shifted the vibrational energies of toluene to (all values in eV) 0.0977, 0.1246, and 0.1280, whereas the energies of the benzene isotopes were chosen as given above. The outcome shows that the overall appearance of the signal, which consists of many single contributions, changes quite a bit. This emphasizes the sensitivity of the CARS signal with respect to the underlying level structure. The main features of the experimental spectrum as shown in Figure 4c, that is, the strong modulation and the decay behavior, are reproduced. Nevertheless, the agreement is far from perfect. We did not try to fit the calculated curves to
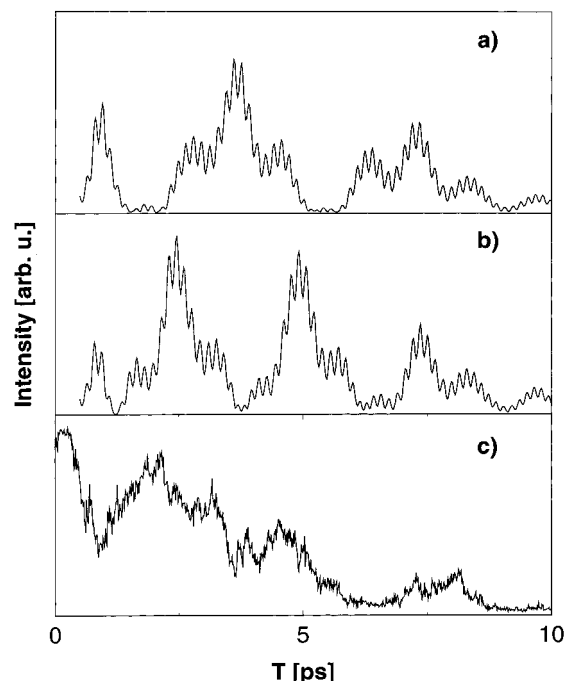
achieve better agreement with experiment and note that our simplified model cannot be expected to give better results.

5. Summary

Femtosecond time-resolved CARS spectroscopy was performed on gas-phase samples of benzene, toluene, and binary mixtures of these molecules. In the case of benzene, a single vibrational state is excited via a nonresonant Raman process. The CARS signal shows no oscillatory patterns and decays within several picoseconds. Perturbative quantum calculations show that the decay is due to the Boltzmann average over many initial rotational states.

For toluene, the two-pulse excitation process results in a coherent superposition of vibrational states. The time-resolved CARS signal shows temporal variations that reflect the vibrational periods of the system. As for benzene, the coherent signal decays on the picosecond time scale because of the dephasing of initially populated rotational levels contributing to the signal. The experimental findings are reproduced by quantum calculations. For a mixture of benzene and toluene, we find a strong oscillation in the transient signal that corresponds to a beat between a vibrational mode excited in benzene and another excited in toluene. This effect is well-known and was detected before in liquid systems. The reason for the interferences between contributions from different molecules in a statistical mixture is the particular measurement performed; the electromagnetic fields emitted by the different molecules are detected so that one measures the coherent superposition of classical electromagnetic fields. The calculations show that the CARS signals are very sensitive to details of the underlying system, i.e., the molecular level structure and the laser field parameters. Thus, time-resolved CARS measurements can provide very detailed information about dynamic molecular processes.

References and Notes

(1) Special issue on Femtochemistry: *J. Phys. Chem.* **1993**, *97*, 12427.

(2) Zewail, A. H. *Femtochemistry*; World Scientific: Singapore, 1994; Vols. 1 and 2.

(3) Manz, J., Wöste, L., Eds. *Femtosecond Chemistry*; VCH: Weinheim, 1995.

(4) Chergui, M., Ed. *Femtochemistry*; World Scientific: Singapore, 1996.

(5) Sundström, V., Ed.; *Femtochemistry and Femtobiology*; World Scientific: Singapore, 1997.

(6) Mukamel, S. *Principles of Nonlinear Optical Spectroscopy*; Oxford University Press: New York, 1995.

(7) Leonhardt, R.; Holzapfel, W.; Zinth, W.; Kaiser, W. *Chem. Phys. Lett.* **1987**, *133*, 373.

(8) Leonhardt, R.; Holzapfel, W.; Zinth, W.; Kaiser, W. *Rev. Phys. Appl.* **1987**, *22*, 1735.

(9) Bron, W. E.; Juhasz, T.; Mehta, S. *Phys. Rev. Lett.* **1989**, *62*, 1655.

(10) Fickenscher, M.; Laubereau, A. *J. Raman Spectrosc.* **1990**, *21*, 857.

(11) Okamoto, H.; Yoshihara, K. *J. Opt. Soc. Am. B* **1990**, *7*, 1702.

(12) Joo, T.; Dugan, M. A.; Albrecht, A. C. *Chem. Phys. Lett.* **1991**, *177*, 4.

(13) Fickenscher, M.; Purucker, H.-G.; Laubereau, A. *Chem. Phys. Lett.* **1992**, *191*, 182.

(14) Kaiser, W., Ed. *Ultrashort Laser Pulses*, 2nd ed.; Springer: Berlin, 1993.

(15) Hayden, C. C.; Chandler, D. W. *J. Chem. Phys.* **1995**, *103*, 10465.

(16) Laubereau, A.; Kaiser, W. *Rev. Mod. Phys.* **1978**, *50*, 607.

(17) Abram, I. I.; Hochstrasser, R. M.; Kohl, J. E.; Semack, M. G.; White, D *J. Chem. Phys.* **1979**, *71*, 153.

(18) Hesp, B. H.; Wiersma, D. A. *Chem. Phys. Lett.* **1980**, *75*, 423.

(19) Dlott, D. D.; Schlosser, C. L.; Chronister, E. L. *Chem. Phys. Lett.* **1982**, *90*, 386.

(20) Ho, F.; Tsay, W. S.; Trout, J.; Hochstrasser, R. M. *Chem. Phys. Lett.* **1981**, *83*, 5.

(21) Zinth, W.; Leonhardt, R.; Holzapfel, W.; Kaiser, W. *IEEE J. Quantum Electron.* **1988**, *QE-24*, 455.

(22) Zinth, W.; Kaiser, W., in ref 14.

(23) Okamoto, H.; Yoshihara, K. *Chem. Phys. Lett.* **1991**, *177*, 568.

(24) Inaba, R.; Okamoto, H.; Yoshihara, K.; Tasumi, M. *Chem. Phys. Lett.* **1991**, *185*, 56.

(25) Purucker, H.-G.; Tunkin, V.; Laubereau, A. *J. Raman Spectrosc.* **1993**, *24*, 453.

(26) Joo, T.; Albrecht, A. C. *Chem. Phys.* **1993**, *176*, 233.

(27) Mukamel, S.; Loring, R. F. *J. Opt. Soc. Am. B* **1986**, *3*, 595.

(28) Mukamel, S. *Annu. Rev. Phys. Chem.* **1991**, *41*, 7806.

(29) Kamalov, V. F.; Svirko, Y. P. *Chem. Phys. Lett.* **1992**, *194*, 1.

(30) Pollard, W. T.; Mathies, R. A. *Annu. Rev. Phys. Chem.* **1992**, *43*, 497.

(31) Hammerich, A. D.; Kosloff, R.; Artner, M. A. *J. Chem. Phys.* **1992**, *97*, 6410.

(32) Ebel, G.; Schinke, R. *J. Chem. Phys.* **1994**, *101*, 1865.

(33) Seidner, L.; Stock, G.; Domcke, W. *J. Chem. Phys.* **1995**, *103*, 3998.

(34) Domcke, W.; Stock, G. *Adv. Chem. Phys.* **1997**, *100*, 1.

(35) Meyer, S.; Schmitt, M.; Materny, A.; Kiefer, W.; Engel, V. *Chem. Phys. Lett.* **1997**, *281*, 332; **1998**, *287*, 753.

(36) Knopp, G.; Schmitt, M.; Materny, A.; Kiefer, W. *J. Phys. Chem.* **1997**, *101*, 4852.

(37) Schmitt, M.; Knopp, G.; Materny, A.; Kiefer, W. *Chem. Phys. Lett.* **1997**, *270*, 9.

(38) Schmitt, M.; Knopp, G.; Materny, A.; Kiefer, W. *J. Phys. Chem. A* **1998**, *102*, 4059.

(39) Maeda, S.; Kamisuki, T.; Adachi, Y. in *Advances in Non-Linear Spectroscopy*; Clark, R. J. H., Hester, R. E., Eds.; Wiley: Chichester, 1988; p 253.

(40) Weast, R. C., Astle, M. J., Eds. *Handbook of Chemistry and Physics*, 61st ed.; CRC Press: Boca Raton, FL, 1981.

(41) Miller, F. A. *J. Raman Spectrosc.* **1988**, *19*, 219.

(42) Herzberg, G. *Molecular Spectra and Molecular Structure*; Krieger Publishing Company: Malabar, 1966; Vol. III.

(43) Zare, R. N. *Angular Momentum*; Wiley: New York, 1988.

(44) Lambert, L. Q.; Compaan, A.; Abella, I. D. *Phys. Rev. A* **1971**, *4*, 2022.